Nonequilibrium discrete nonlinear Schrödinger equation

Stefano Iubini,[1,2] Stefano Lepri,[1,*] and Antonio Politi[3,1]

[1]*Consiglio Nazionale delle Ricerche, Istituto dei Sistemi Complessi, via Madonna del Piano 10, I-50019 Sesto Fiorentino, Italy*
[2]*Dipartimento di Fisica e Astronomia, Università di Firenze and INFN Sezione di Firenze, via Sansone 1, I-50019 Sesto Fiorentino, Italy*
[3]*Institute for Complex Systems and Mathematical Biology & SUPA University of Aberdeen, Aberdeen AB24 3UE, United Kingdom*

We study nonequilibrium steady states of the one-dimensional discrete nonlinear Schrödinger equation. This system can be regarded as a minimal model for the stationary transport of bosonic particles such as photons in layered media or cold atoms in deep optical traps. Due to the presence of two conserved quantities, namely, energy and norm (or number of particles), the model displays coupled transport in the sense of linear irreversible thermodynamics. Monte Carlo thermostats are implemented to impose a given temperature and chemical potential at the chain ends. As a result, we find that the Onsager coefficients are finite in the thermodynamic limit, i.e., transport is normal. Depending on the position in the parameter space, the "Seebeck coefficient" may be either positive or negative. For large differences between the thermostat parameters, density and temperature profiles may display an unusual nonmonotonic shape. This is due to the strong dependence of the Onsager coefficients on the state variables.

I. INTRODUCTION

The discrete nonlinear Schrödinger (DNLS) equation [1,2] has important applications in many domains of physics. As is well known, such an equation arises in several different problems. A classical example is electronic transport in biomolecules [3]. In the context of optics or acoustics, it describes the propagation of nonlinear waves in a layered photonic or phononic system. Indeed, in a suitable limit, the dynamics of high-frequency Bloch waves is described by a DNLS equation for their envelope (see Refs. [4,5] for details). On the other hand, in the realm of the physics of cold atomic gases, the equation is an approximate semiclassical description of bosons trapped in periodic optical lattices (see, e.g., Ref. [6] and references therein for a recent survey). Many other physical problems have been recently addressed having the DNLS equation as a basic reference model, such as the effect of nonlinearity on Anderson localization [7,8] and the violation of reciprocity in wave scattering [9], just to mention a few recent examples.

While a vast literature has been devoted to localization problems, much less is known about finite-temperature properties. An analysis of the equilibrium statistical mechanics of the continuous nonlinear Schrödinger equation was presented in Ref. [10]. The discrete case was considered more recently in Ref. [11], while the relaxation of localized modes (discrete breathers) in the presence of phonon baths has been discussed in Refs. [12,13]. Several results can be translated to other types of nonlinear lattices, where a DNLS-like equation represents an approximation of the lattice dynamics [14].

An even less explored field is that of nonequilibrium properties of the DNLS equation. The relaxation to equilibrium of the nonlinear Schrödinger equation with saturated, focusing nonlinearity has been studied in Ref. [15], where the evolution was projected over a finite number of Fourier modes (as

opposed to the spatial discretization of the DNLS case), finding numerical evidence of slow relaxation and metastability.

However, the case of an open system that steadily exchanges energy with external reservoirs has not been treated so far. The presence of two conserved quantities naturally requires one to argue about coupled transport, in the sense of ordinary linear irreversible thermodynamics. Despite the very many studies of heat conduction in oscillator chains [16,17], works on coupled transport are scarce [18–21]. Interest in this field has been revived by recent works on thermoelectric phenomena [22,23] in the hope of identifying dynamical mechanisms that could enhance the efficiency of thermoelectric energy conversion [24,25].

In order to investigate transport properties, we need to introduce the interaction of the system with external reservoirs that are capable to exchange energy and/or norm. For models like DNLS, this is much less straightforward than for standard oscillator chains, where, e.g., Langevin thermostats are a typical choice [16,17]. Here we propose and test a very simple Monte Carlo scheme which is easy to implement and suitable for the model at hand. Another important difference between the DNLS and standard oscillator chains (like the Fermi-Pasta-Ulam or Klein-Gordon models) is that its Hamiltonian is not the sum of kinetic and potential energies. Thus, it is necessary to introduce suitable operative definitions of kinetic temperature T and chemical potential μ to measure such quantities in actual simulations. In the following, we make use of a recent definition of the microcanonical temperature [26] and extend it for the estimate of the chemical potential.

By imposing small T and μ jumps across the chain, we can determine the Onsager coefficients, which turn out to be finite in the thermodynamic limit, i.e., both energy and mass conductions are normal processes. From the Onsager coefficients, we can thereby determine the "Seebeck coefficient" S [27], which we find to be either positive or negative depending on the thermodynamic parameters (i.e., mass and energy density). For larger temperature or chemical-potential differences, although one can still invoke the linear response theory, some surprising phenomena emerge. One example is the "anomalous heating"

_____
*stefano.lepri@isc.cnr.it

that can be observed when the chain is attached to two thermostats operating at the same temperature: along the chain, T reaches values that are as much as three times larger than that imposed on the boundaries. This phenomenon can be observed only in the case of coupled transport, since it is due to the variable weight of the nondiagonal terms of the Onsager matrix. It is apparent in the DNLS because of the strong variability of the Onsager coefficients.

The paper is organized as follows. In Sec. II, we introduce the model and describe the heat baths. In Sec. III, we define the relevant thermodynamic observables and the formalism (e.g., the Onsager coefficients) necessary to characterize nonequilibrium steady states. Section IV is devoted to a discussion of the steady states, both in the case of small and large T, μ differences. In Sec. V, we provide a pictorial representation of the general transport properties by reconstructing the zero-flux curves. Finally, the last section is devoted to the conclusions and to a brief summary of the open problems.

II. SETUP

In one dimension, the DNLS Hamiltonian writes

$$H = \frac{1}{4} \sum_{i=1}^{N} \left(p_i^2 + q_i^2 \right)^2 + \sum_{i=1}^{N-1} (p_i p_{i+1} + q_i q_{i+1}), \qquad (1)$$

where the sum runs over the N sites of the chain. The sign of the quartic term is positive, as we refer to a repulsive-atom BEC, while the sign of the hopping term is irrelevant due to the symmetry associated with the canonical (gauge) transformation $z_n \rightarrow z_n e^{i\pi n}$ (where $z_n \equiv (p_n + \iota q_n)/\sqrt{2}$ denotes the amplitude of the wave function). The equations of motion are

$$i\dot{z}_n = -z_{n+1} - z_{n-1} - 2|z_n|^2 z_n, \qquad (2)$$

with $n = 1, \ldots, N$, and fixed boundary conditions ($z_0 = z_{N+1} = 0$). The model has two conserved quantities, namely, the energy and the total norm (or total number of particles),

$$A = \sum_{i=1}^{N} \left(p_i^2 + q_i^2 \right). \qquad (3)$$

As a consequence, the equilibrium phase diagram is two dimensional, as it involves the energy density $h = H/N$ and the particle density $a = A/N$. A reconstruction of the diagram was carried out in Ref. [11] within the grand-canonical ensemble with the help of transfer integral techniques. It is schematically described in Fig. 1: the lower dashed line corresponds to the ground state ($T = 0$) upon varying the particle density, and the upper dashed line corresponds to infinite temperature. The nonequilibrium studies described in this paper correspond to the region in between two such curves.

We aim to characterize the steady states of the chain when put in contact (on the left and right boundaries) with two thermostats at temperature T_L and T_R and chemical potentials μ_L and μ_R, respectively. The implementation of the interactions with a heat bath is often based on heuristics. In particle models, the simpler schemes consist of either adding a Langevin noise or assuming random collisions with an equilibrium gas [16,17]. For the DNLS, this is less straightforward: adding white noise and a linear dissipation
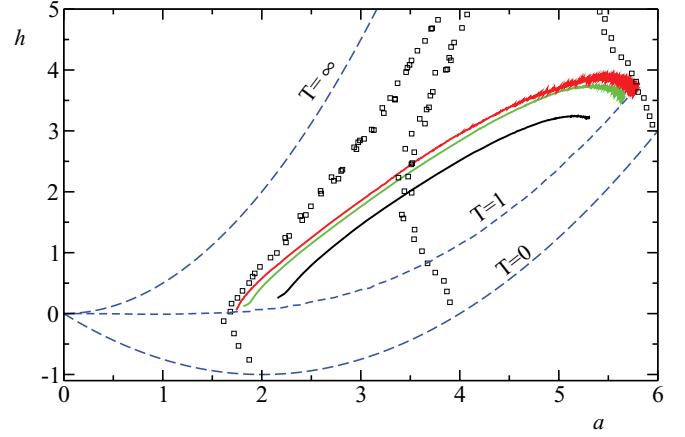

FIG. 1. (Color online) Parametric plots of the local norm and energies $[a(y), h(y)]$ for $T_L = T_R = 1$, $\mu_L = 0$, $\mu_R = 2$ and increasing chain lengths $N = 200, 800, 3200$ (solid lines, bottom to top). The three (blue) dashed lines are the isothermal $T = 0$, $T = 1$, and $T = \infty$, respectively. Lines at constant chemical potential (open symbols) $\mu = 0$, $\mu = 1$, and $\mu = 2$ (left to right, respectively) are obtained by equilibrium simulations.

drives the system to infinite temperature, i.e., to a state in which relative phases are uncorrelated [28].

In the absence of a first-principles definition of heat bath, we consider two phenomenological Monte Carlo heat baths. The general scheme of this kind of heat bath involves a stochastic dynamics, which perturbs the canonical variables $p_1 \rightarrow p_1 + \delta p_1$ and $q_1 \rightarrow q_1 + \delta q_1$ [30] at random times, chosen according to a uniform distribution in the interval $[t_{\min}, t_{\max}]$. The perturbations δp and δq are independent random variables uniformly distributed in the interval $[-R, R]$. Moves are accepted according to the standard Metropolis algorithm, evaluating the cost function $\exp\{-T_L^{-1}(\Delta H - \mu_L \Delta A)\}$, with T_L and μ_L being the temperature and the chemical potential of the heat bath. This kind of thermostat exchanges both energy and particles. In some cases, however, we need to study the chain behavior in the absence of one of the two fluxes (energy and norm). A simple way to study these setups is to modify the perturbation rule of the thermostat, requiring the exact conservation of the corresponding local density (energy density or norm density). We have thus the following two schemes:

Norm-conserving thermostat—The perturbation acts only on the phase ϕ_1 of the complex variable z_1. More precisely we impose $\phi_1 \rightarrow \phi_1 + \delta\phi_1 \bmod(2\pi)$, where $\delta\phi_1$ is a random variable, uniformly distributed in the interval $[0, 2\pi]$. This dynamics conserves exactly the local amplitude $|z_1|^2$ and therefore the total norm A.

Energy conserving thermostat—In this case, it is necessary to go through two steps to conserve the energy,

$$e_1 = |z_1|^4 + 2|z_1||z_2| \cos(\phi_1 - \phi_2). \qquad (4)$$

First, the amplitude $|z_1|$ is randomly perturbed. As a result, both the local amplitude and the local energy change. Then, by inverting, Eq. (4), a value of ϕ_1 that restores the initial energy is sought. If no such solution exists, we go back to the first step and choose a new perturbation for $|z_1|$.

As a first test of the Monte Carlo dynamics, we verified that the $T = $ const and $\mu = $ const lines are correctly reproduced at equilibrium, i.e., for $T_L = T_R$ and $\mu_L = \mu_R$ (see, e.g., the open symbols in Fig. 1). In particular, the $\mu = 0$ line is in accordance with the curve computed with the transfer integral method (see Fig. 1 in Ref. [11]), as well as with the approximate analytical expression given in Ref. [29]. Notice that both sets of curves are not monotonous in the (a,h) plane, indicating the presence of a nontrivial relation between the energy-norm parametrization and the temperature-chemical potential one.

There is a basic difference between the two types of thermostats. In the general scheme, a steady state is characterized by four parameters T_L, T_R, μ_L, and μ_R. On the other hand, for the norm-conserving scheme, we only assign T_L, T_R and the norm density a_{tot} of the whole chain. As a consequence, the value of μ on the boundary is not fixed and must be computed from the simulation. If the steady state is unique, the former thermostating scheme must yield the same results once the chemical potentials are suitably fixed. A numerical test of this equivalence has been performed by reconstructing some zero-flux profiles with both thermostats. The curves overlap reasonably well, although some small systematic deviations are present. This is because the norm flux is never exactly zero in the nonconservative case (typically of the order of $\sim 10^{-4}$ in a chain of 1000 sites). In addition, there are slightly different thermal resistance effects in the two schemes. Besides those discrepancies, we conclude that the proposed schemes work equally well for the generation of nonequilibrium steady states.

As usual in nonequilibrium molecular dynamics simulations, some tuning of the bath parameters is required to minimize boundary resistance and decrease the statistical errors, as well as the finite-size effects [16]. For our Monte Carlo thermostats, we observed that it is necessary to tune the perturbation amplitude R. Typically, there is an optimal value of R for which one of the two currents is maximal (keeping the other parameters fixed), but this value may depend on T and μ. Since it would be impractical to tune the thermostat parameters in each simulation, we decided to fix them in most of the cases. In particular we have chosen $R = 0.5$, $t_{\min} = 10^{-2}$, and $t_{\max} = 10^{-1}$. Some adjustments have been made only when the fluxes were very small.

III. PHYSICAL OBSERVABLES

In order to characterize the thermodynamic properties of the DNLS, we extend the approach of Ref. [26] to derive an operative definition not only of the microcanonical temperature but also of the chemical potential. The starting point is the usual definitions $T^{-1} = \partial\mathcal{S}/\partial H$ and $\mu/T = -\partial\mathcal{S}/\partial A$, where $\mathcal{S}$ is the thermodynamic entropy. The partial derivatives must be computed taking into account the existence of two conserved quantities (hereafter called C_1 and C_2). Thus,

$$\frac{\partial\mathcal{S}}{\partial C_1} = \left\langle \frac{W\|\vec{\xi}\|}{\vec{\nabla}C_1 \cdot \vec{\xi}} \; \vec{\nabla} \cdot \left(\frac{\vec{\xi}}{\|\vec{\xi}\|W} \right) \right\rangle, \tag{5}$$

where $\langle\cdot\rangle$ stands for the microcanonical average,

$$\vec{\xi} = \frac{\vec{\nabla}C_1}{\|\vec{\nabla}C_1\|} - \frac{(\vec{\nabla}C_1 \cdot \vec{\nabla}C_2)\vec{\nabla}C_2}{\|\vec{\nabla}C_1\|\|\vec{\nabla}C_2\|^2},$$

$$W^2 = \sum_{\substack{j,k=1 \\ j<k}}^{2N} \left[\frac{\partial C_1}{\partial x_j}\frac{\partial C_2}{\partial x_k} - \frac{\partial C_1}{\partial x_k}\frac{\partial C_2}{\partial x_j} \right]^2, \tag{6}$$

and $x_{2j} = q_j$, $x_{2j+1} = p_j$. By setting $C_1 = H$ and $C_2 = A$, the above formula reduces to the expression for T derived in [26]. Moreover, by assuming $C_1 = A$ and $C_2 = H$, Eq. (5) defines the chemical potential μ. Notice that both expressions are nonlocal. Nevertheless, we have verified that it is sufficient to compute the expression (5) over as few as ten sites to obtain, after some time averaging, reliable "local" estimates of both T and μ [31].

The expressions for the local energy and particle fluxes are derived in the usual way from the continuity equations for norm and energy densities, respectively,

$$j_a(n) = 2(p_{n+1}q_n - p_nq_{n+1}), \tag{7}$$

$$j_h(n) = -(\dot{p}_np_{n-1} + \dot{q}_nq_{n-1}). \tag{8}$$

The approach to the steady state is controlled by verifying that the (time) average fluxes are constant along the chain $[\overline{j_a(n)} = j_a$ and $\overline{j_h(n)} = j_h]$. Moreover, it is also checked that j_a and j_h are, respectively, equal to the average energy and norm exchanged per unit time with the reservoirs.

In the thermodynamic limit (i.e., for sufficiently long chains), the local forces acting on the system are very weak and one can thereby invoke the linear response theory. This means that forces and fluxes are related by the relations [25]

$$j_a = -L_{aa}\frac{d(\beta\mu)}{dy} + L_{ah}\frac{d\beta}{dy},$$

$$j_h = -L_{ha}\frac{d(\beta\mu)}{dy} + L_{hh}\frac{d\beta}{dy}, \tag{9}$$

where we have introduced the continuous variable $y = i/N$, while β denotes the inverse temperature $1/T$; $\mathbf{L}$ is the symmetric, positive definite, 2×2 Onsager matrix. Notice that the first term in the right-hand side of the above equations is negative, since the thermodynamic forces are $-\beta\mu$ and μ, and $\det\mathbf{L} = L_{aa}L_{hh} - L_{ha}^2 > 0$.

The particle (σ) and thermal (κ) conductivity can be expressed in terms of $\mathbf{L}$,

$$\sigma = \beta L_{aa}, \quad \kappa = \beta^2\frac{\det\mathbf{L}}{L_{aa}}. \tag{10}$$

Analogously, the Seebeck coefficient S, which corresponds to (minus) the ratio between the chemical-potential gradient and the temperature gradient (in the absence of a mass flux), writes

$$S = \beta\left(\frac{L_{ha}}{L_{aa}} - \mu\right). \tag{11}$$

We conclude this section by mentioning another important parameter, namely, the figure of merit

$$ZT = \frac{\sigma S^2 T}{\kappa} = \frac{(L_{ha} - \mu L_{aa})^2}{\det\mathbf{L}},$$

which determines the efficiency η for the conversion of a heat current into a particle current as [25]

$$\eta = \eta_C \frac{\sqrt{ZT + 1} - 1}{\sqrt{ZT + 1} + 1}.$$

For large ZT, η approaches the Carnot limit η_C. Understanding the microscopic mechanisms leading to an increase of ZT is currently an active topic of research [22].

IV. STEADY STATES

A. Local analysis

In a first series of simulations, we have studied the nonequilibrium states in the case of small differences between the two thermostats, verifying that transport is normal, i.e., the Onsager coefficients are finite in the thermodynamic limit. This is less obvious than one could have imagined [32]. In any case, for fixed $\Delta T = T_R - T_L$ and $\Delta\mu = \mu_R - \mu_L$, the two fluxes j_a and j_h are inversely proportional to the system size N. At high enough temperatures, the asymptotic scaling sets in already in chains a few hundred sites long [see Fig. 2(a)]. Moreover, if ΔT and $\Delta\mu$ are small enough, the profiles of T and μ along the chain are linear as expected.

However, upon decreasing the temperature, the minimal chain length needed to observe a normal transport becomes very large. As shown in Fig. 2(b), for the same range of lattice sizes as in Fig. 2(a), the currents are almost independent on N, as one would expect in the case of ballistic transport. This is because, at small temperatures, one can always linearize the equations of motion around the ground state (which depends on the norm density), obtaining a harmonic description and thereby an integrable dynamics.

A plot of the four Onsager coefficients in the (T,μ) plane is reported in Fig. 3. Within statistical errors, the off-diagonal terms are always positive in the considered range.
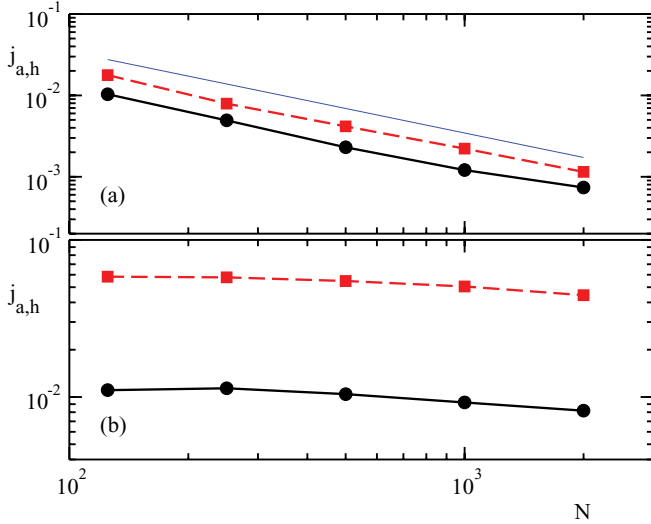

FIG. 2. (Color online) Average energy current (squares) and norm current (dots) vs chain size N: (a) High-temperature regime $T_L = 2$, $T_R = 4$, $\mu = 0$, and (b) low-temperature regime $T_L = 0.3$, $T_R = 0.7$, $\mu = 1.5$. The thin (blue) line is the $1/N$ behavior expected for normal transport. Each value is obtained by computing the fluxes on a run of 5×10^6 time units.
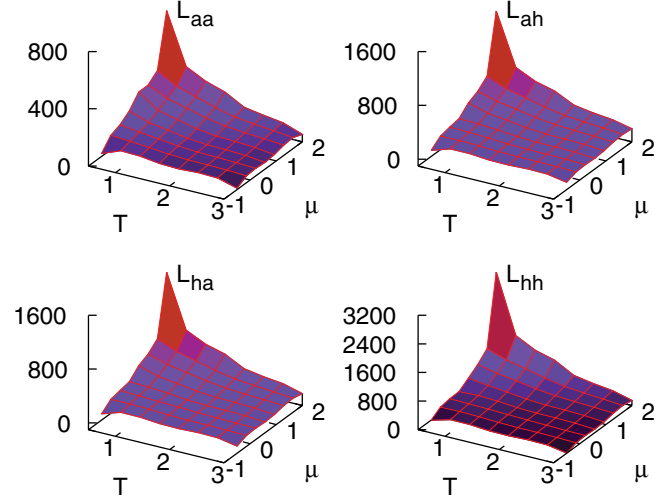

FIG. 3. (Color online) Elements of the Onsager matrix **L** in the T,μ plane for a chain of length $N = 500$; $\Delta T = 0.1$, $\Delta\mu = 0.05$. Each value is obtained by computing the fluxes on a run of 5×10^6 time units.

All coefficients are larger for small T and large μ. This is connected to the scaling behavior of the linear coefficients in the vicinity of the ground state [32].

The resulting coefficient S is plotted in Fig. 4(a), where one can see that there are two regions where the Seebeck coefficient has different sign, separated by a curve which, according to Eq. (11), is defined by $L_{ha}/L_{aa} = \mu$ (see below). This means that the relative sign of the temperature and chemical-potential gradients is opposite in the two regions (in the presence of a zero norm flux). This is indeed seen in Fig. 4(b), where the result of two different simulations are plotted in the two regions.

Finally, since the figure of merit ZT roughly follows S, there is only a modest change in the considered parameter ranges. Moreover, for fixed T, ZT decreases upon increasing μ. This is qualitatively in agreement with the general expectation that an increasing strength of interaction (increasing μ means increasing the average norm and thus the nonlinearity) is detrimental for the efficiency.

B. Global analysis

If the temperature or the chemical-potential difference is no longer small, then the temperature and chemical-potential profiles are expected to have a nonlinear shape. This is because, as we have seen in the previous section, the Onsager matrix varies with a and h (or, equivalently, with T and μ).

A particularly striking example is reported in Fig. 5. Both $T(y)$ and $\mu(y)$ profiles do approach the imposed values at the chain edges (up to tiny jumps due to the boundary impedance). However, $T(y)$ exhibits a remarkable nonmonotonous profile: although the chain is attached to two heat baths with the same temperature, it is substantially hotter in the middle (up to a factor 3!).

Another way to represent the data is by plotting the local norm and energy densities in the phase plane (a,h). By comparing the results for different chain lengths, we see in Fig. 1 that the paths are progressively "pushed" away from the
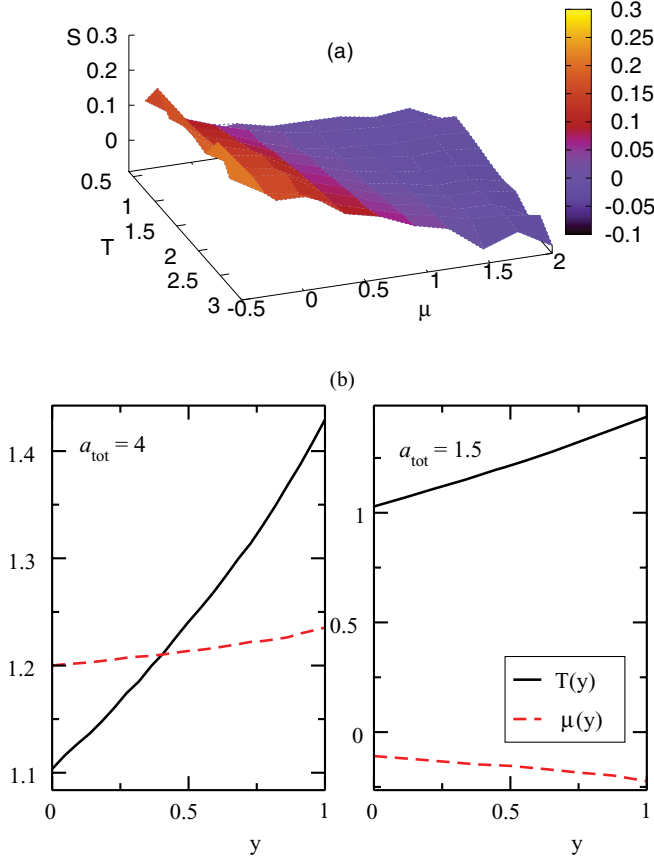
FIG. 4. (Color online) (a) Seebeck coefficient S obtained from the data in Fig. 3; (b) Temperature and chemical-potential profiles for $T_L = 1$, $T_R = 1.5$; simulation with norm-conserving thermostats at two values of the norm density a_{tot} corresponding to values of S with opposite signs.

$T = 1$ isothermal and, for $N = 3200$, the asymptotic regime is attained.

In order to understand the onset of such anomalous shape, it is convenient to rewrite Eq. (9) by referring to T and μ. By introducing vector notations, we can write

$$\mathbf{J} = \mathbf{A}(\mu, T)\frac{d\mathbf{v}}{dy}, \qquad (12)$$

where $\mathbf{J} = (j_a, j_h)$, $\mathbf{v} = (\mu, T)$, while the matrix $\mathbf{A}$ (which is no longer symmetric) can be expressed in terms of the Onsager matrix and of the fields T and μ (for instance, $A_{11} = -L_{aa}/T$). Inverting the above equation, one obtains

$$\frac{d\mathbf{v}}{dy} = \mathbf{A}^{-1}(\mu, T)\mathbf{J}, \qquad (13)$$

where $\mathbf{A}^{-1}$ denotes the inverse of $\mathbf{A}$. This system describes a set of two linear differential equations which are nonautonomous (since the matrix coefficients in general vary with μ and T).

If one assumes to know the "material" properties (i.e., the matrix $\mathbf{A}^{-1}$) and wishes to determine fluxes and profiles, one can proceed by integrating the differential equations, starting from the initial condition $T(0) = T_L$, $\mu(0) = \mu_L$. The *a priori* unknown parameters j_a and j_h can be determined by imposing that the final condition is $T(1) = T_R$ and $\mu(1) = \mu_R$.
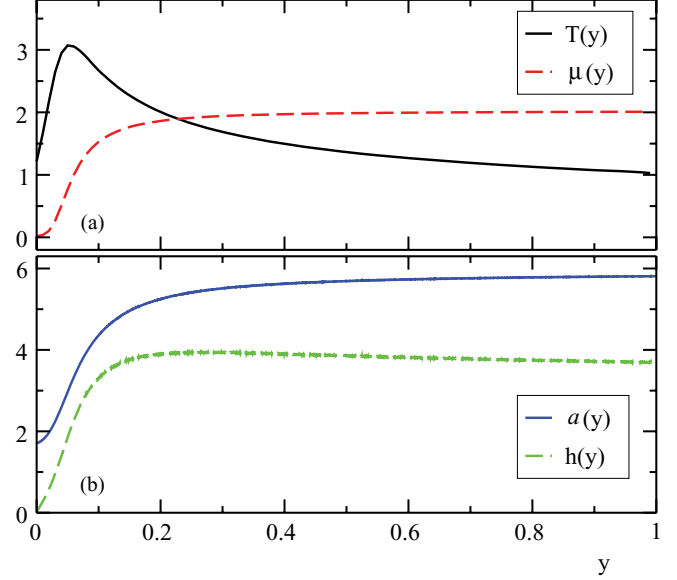

FIG. 5. (Color online) (a) Temperature and chemical-potential profiles as a function of $y = i/N$ for a chain of $N = 3200$ sites and $T_L = T_R = 1$, $\mu_L = 0$, $\mu_R = 2$. Each point is an average of the appropriate microcanonical expression derived from Eq. (5) over a subchain of about ten sites around i. (b) Norm and energy densities corresponding to the profiles in (a).

Alternatively, if the fluxes are known, one can integrate the equations up to any point y_0, and thereby generate the profiles that would be obtained by attaching the right end of the chain to thermal baths with temperature $T_R = T(y_0)$ and chemical potential $\mu_R = \mu(y_0)$.

In order to check the validity of the method, we have also adopted an alternative point of view by combining the knowledge of the fluxes with simulations of short chains and small gradients to determine the elements of the matrix $\mathbf{A}$ in suitably selected points in the (T, μ) plane. In order to estimate the four entries of $\mathbf{A}$, it is necessary to perform two independent simulations for

$$\begin{cases} T_{L,R} = T \pm \Delta T \\ \mu_{L,R} = \mu \end{cases} \qquad \begin{cases} T_{L,R} = T \\ \mu_{L,R} = \mu \pm \Delta\mu. \end{cases}$$

With such information, we have been able to estimate $d\mathbf{v}/dy$ along the chain [from Eq. (13)] and to compare the results with the direct simulations. The results plotted in Fig. 6 demonstrate that the two approaches are in excellent agreement.

V. ZERO FLUX CURVES

A compact pictorial representation of transport properties is obtained by drawing the lines corresponding to vanishing fluxes j_a and j_h. They can be directly determined by means of the conservative thermostats presented in Sec. II. Some lines are plotted in Fig. 7, both in the plane (a, h) and (T, μ). It is worth recalling that in the absence of a mutual coupling between the two transport processes (zero off-diagonal elements of the Onsager matrix), such curves would be vertical and horizontal lines in the latter representation. It is instead remarkable to notice that the solid lines, which correspond to $j_h = 0$, are almost vertical for large μ: this means that in spite of a large temperature difference, the energy flux is very small.
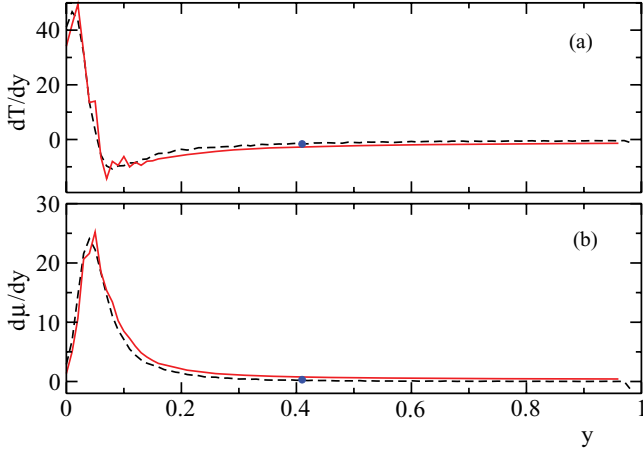
FIG. 6. (Color online) Spatial derivatives of T and μ [panels (a) and (b), respectively] computed from the profiles of Fig. 5 (black dashed lines) and their reconstruction (red solid lines) by Eq. (13) using the linear response coefficients (matrix **A**). The latter have been calculated on a chain of $N = 250$. The quality of the reconstruction improves by increasing the lattice size as shown by the blue filled dot which is obtained for $N = 1000$.

This is an indirect but strong evidence that the nondiagonal terms are far from negligible.

The condition of a vanishing particle flux $j_a = 0$ defines the Seebeck coefficient, which is $S = -d\mu/dT$. Accordingly, the points where the dashed curves are vertical in Fig. 7(b) identify the locus where S changes sign. The $j_h = 0$ curves have no direct interpretation in terms of standard transport coefficients. Finally, if one connects a DNLS chain with any two points in the (μ, T) plane, its profile would correspond to the only path that is characterized by a constant ratio of j_a/j_h.

It is instructive to compare these results with the scenario expected in the "harmonic" limit, where the nonlinear terms in the DNLS are negligible. Here, the dynamics is characterized by an ensemble of freely propagating waves, and transport is thus ballistic. A direct reconstruction of the zero-flux lines by direct simulations is not very useful, as, in analogy with the known behavior for the harmonic chain [33], the profiles of T and μ are flat (except for a few sites close to the boundaries). Thus, the curves degenerate to single points and no comparison is possible. We thus resort to a different method of computing transport coefficients for ballistic systems, which is completely analogous to the well-known Landauer theory of electronic transport [34]. Consider an N-site chain in between two leads at different temperatures and chemical potentials (T_L, μ_L), (T_R, μ_R). Since transport is ballistic, energy and norm are carried by N independent phonon modes, whose dispersion law is $\omega(q) = 2\cos q$, with q being the wave number ($|q| \leqslant \pi$). Accordingly, the fluxes are N independent and the ensuing transport coefficients are proportional to N. In this context, the norm and energy fluxes are given (up to some numerical constant) by the formulas

$$J_a = \int_{-2}^{+2} d\omega \, t(\omega)[f_L(\omega) - f_R(\omega)],$$

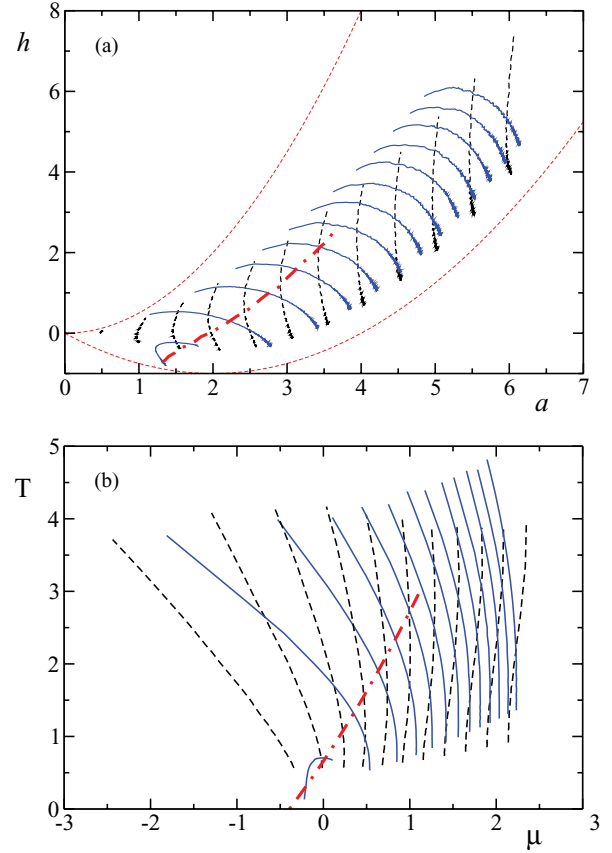$$J_h = \int_{-2}^{+2} d\omega \, \omega \, t(\omega) [f_L(\omega) - f_R(\omega)],$$

FIG. 7. (Color online) Zero-flux curves in the (a,h) and (μ, T) planes [panels (a) and (b), respectively]. Black dashed lines correspond to $j_a = 0$ and are obtained with norm-conserving thermostats upon fixing the total norm density a_{tot}, T_L, and T_R. Blue solid lines are for $j_h = 0$ using energy-conserving thermostats with fixed total energy density h_{tot}, μ_L/T_L, and μ_R/T_R. Simulations are for a chain of length $N = 500$. The thin dashed lines in the upper panel are the $T = 0$ and $T = \infty$ isothermals. The thick dot-dashed lines identify the locus where S changes sign (see text).

where $t(\omega)$ denotes the transmission coefficient, while $f_{L,R}$ are the equilibrium distribution functions of the reservoirs. If we assume that they are composed of two infinite linear chains (both with the same dispersion), then the equipartition principle implies that the distributions are of the Rayleigh-Jeans form [13] $f_{L,R}(\omega) = f(T_{L,R}, \mu_{L,R}, \omega)$, where

$$f(T, \mu, \omega) = \frac{T}{\omega - 2\mu}$$

[the factor 2 stems from the definition of z_n and Eq. (3)]. The physical meaning of the formulas is pretty intuitive: they can be derived from suitable generalized Langevin equations [32] following similar steps as for coupled oscillators; see, e.g., Ref. [35]. The relevant information is contained in the transmission coefficient that depends on how the chain is coupled to the external leads. For the Monte Carlo bath, throughout this paper, the precise form of t is not known. We thus postulate the simplest possible form, namely, that for large N, $t(\omega) = t$ for $|\omega| < 2$, and zero otherwise. For our purposes, we set $t = 1$ in the following, otherwise all of the coefficients
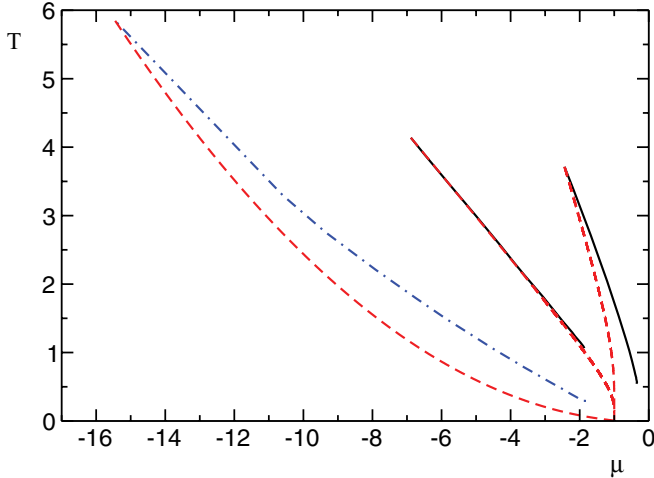
FIG. 8. (Color online) Comparison of the zero-flux lines obtained from simulation of the DNLS equations (black solid and blue dot-dashed lines correspond to $j_a = 0$ and $j_h = 0$, respectively). The red dashed lines are the zero-flux lines computed by the Landauer formulas as described in the text.

must be multiplied by t. If we introduce the function

$$\Phi(T,\mu) \equiv \int_{-2}^{+2} d\omega \, f(T,\mu,\omega) = T \ln\left(\frac{\mu-1}{\mu+1}\right),$$

which for $\mu < -1$ and $T > 0$ is always positive, then we can write

$$J_a = \Phi(T_L,\mu_L) - \Phi(T_R,\mu_R),$$
$$J_h = 4(T_L - T_R) + 2\mu_L\Phi(T_L,\mu_L) - 2\mu_R\Phi(T_R,\mu_R).$$

By expanding to first order in $\Delta T = (T_L - T_R)$ and $\Delta\mu = (\mu_L - \mu_R)$,

$$\begin{aligned} J_a &= M_{00}\Delta T + M_{01}\Delta\mu, \\ J_h &= M_{10}\Delta T + M_{11}\Delta\mu, \end{aligned} \qquad (14)$$

where

$$\mathbf{M} = \begin{pmatrix} \frac{\Phi(T,\mu)}{T} & \frac{2T}{\mu^2-1} \\ 4 + \frac{2\mu\Phi(T,\mu)}{T} & \frac{4T\mu}{\mu^2-1} + 2\Phi(T,\mu) \end{pmatrix}.$$

With the help of the explicit formulas (14), we can reconstruct the zero-flux curves as follows. Starting from an initial point $(T_{\text{in}},\mu_{\text{in}})$, we compute ΔT and $\Delta\mu$ inverting Eqs. (14) setting $J_a = 0, J_h = 1$ and $J_a = 1, J_h = 0$, respectively (the value 1 is arbitrary). We then let $(T_{\text{in}},\mu_{\text{in}}) \rightarrow (T_{\text{in}} + \Delta T, \mu_{\text{in}} + \Delta\mu)$ and iterate the procedure until the whole lines are reconstructed.

The results are depicted in Fig. 8. The curves for the linear case are defined only in the region $\mu < -1$. The results of the simulations of the DNLS (solid lines) nicely approach the curves of the linear case (dashed lines) upon decreasing μ. The agreement is satisfactory, especially in view of the many *ad hoc* assumptions made in deriving Eqs. (14).

VI. CONCLUSIONS

We have presented a study of stationary thermal transport properties in the DNLS equation. Due to the nonstandard form of its Hamiltonian, several new issues have been brought to the fore dealing with energy transport in oscillator chains. In particular, we have extended the microscopic definition of the temperature to the chemical potential and defined suitable Monte Carlo thermostating schemes to characterize the nonequilibrium steady states of the DNLS in various regimes. The simulations confirm the expectations that transport is normal (i.e., the Onsager coefficients are finite in the thermodynamic limit), although some almost ballistic transport is found at very low temperature, where the DNLS approaches an almost integrable limit.

Due to the very existence of two naturally coupled transport processes, the nonequilibrium steady state can display nonmonotonous energy and density profiles, which is an unusual feature for an oscillator or particle model. As seen from Eq. (13), it is clear that the temperature profile cannot in general be linear in y, since the elements of $\mathbf{A}^{-1}$ depend on μ and T. In principle, the profiles may have nontrivial shapes depending on the qualitative behavior of the solutions of Eq. (13). In the DNLS, the phenomenon is particularly pronounced (the temperature inside the chain reaches values that are almost three times larger than those imposed by the thermal baths) because of the strong variability of the Onsager coefficients. It would be interesting to find the physical motivation for this effect to predict and possibly control the conditions for its appearance.

Another feature is the fact that the Seebeck coefficient changes sign upon changing the state parameters, e.g., by increasing the interaction strength. The observable consequence of this is that the temperature and chemical-potential gradients change their relative signs. Thus, there are situations in which the particle density a may be larger in the colder regions.

Furthermore, a remarkable feature of the DNLS thermodynamics is the possibility of negative temperature states in suitable parameter regions [11]. These regions, which are characterized by the presence of long-lived localized excitations (discrete breathers), have not be considered in the present paper, but are definitely worth being explored. It may be indeed speculated that they would lead to genuine nonlinear transport features and even to the birth of new dynamical regimes possibly displaying transitions between conducting and insulating states.

Besides its intrinsic theoretical interest as a test bed for the characterization of coupled irreversible processes, the DNLS equation opens the way also to experimental investigations. In fact, despite its mathematical simplicity, the DNLS model can be of guidance in the design and interpretation of experiments on coupled transport in cold atomic gases in deep optical lattices as well as in optical multilayered and nonlinear structures.

[1] J. Eilbeck, P. Lomdahl, and A. Scott, Physica D **16**, 318 (1985).

[2] P. G. Kevrekidis, *The Discrete Nonlinear Schrödinger Equation* (Springer Verlag, Berlin, 2009).

[3] A. Scott, *Nonlinear Science. Emergence and Dynamics of Coherent Structures* (Oxford University Press, Oxford, 2003).

[4] A. M. Kosevich and M. A. Mamalui, J. Exp. Theor. Phys. **95**, 777 (2002).

[5] G. Tsironis and D. Hennig, Phys. Rep. **307**, 333 (1999).

[6] R. Franzosi, R. Livi, G. Oppo, and A. Politi, Nonlinearity **24**, 89R (2011).

[7] G. Kopidakis, S. Komineas, S. Flach, and S. Aubry, Phys. Rev. Lett. **100**, 084103 (2008).

[8] A. S. Pikovsky and D. L. Shepelyansky, Phys. Rev. Lett. **100**, 094101 (2008).

[9] S. Lepri and G. Casati, Phys. Rev. Lett. **106**, 164101 (2011).

[10] J. L. Lebowitz, H. A. Rose, and E. R. Speer, J. Stat. Phys. **50**, 657 (1988).

[11] K. Ø. Rasmussen, T. Cretegny, P. G. Kevrekidis, and N. Grønbech-Jensen, Phys. Rev. Lett. **84**, 3740 (2000).

[12] K. Ø. Rasmussen, S. Aubry, A. Bishop, and G. Tsironis, Eur. Phys. J. B **15**, 169 (2000).

[13] B. Rumpf, Phys. Rev. E **69**, 016618 (2004).

[14] M. Johansson, Physica D **216**, 62 (2006).

[15] A. Eisner and B. Turkington, Physica D **213**, 85 (2006).

[16] S. Lepri, R. Livi, and A. Politi, Phys. Rep. **377**, 1 (2003).

[17] A. Dhar, Adv. Phys. **57**, 457 (2008).

[18] M. Gillan and R. Holloway, J. Phys. C **18**, 5705 (1985).

[19] C. Mejia-Monasterio, H. Larralde, and F. Leyvraz, Phys. Rev. Lett. **86**, 5417 (2001).

[20] H. Larralde, F. Leyvraz, and C. Mejía-Monasterio, J. Stat. Phys. **113**, 197 (2003).

[21] D. Basko, Ann. Phys. **326**, 1577 (2011).

[22] G. Casati, C. Mejía-Monasterio, and T. Prosen, Phys. Rev. Lett. **101**, 016601 (2008).

[23] G. Casati, L. Wang, and T. Prosen, J. Stat. Mech.: Theory Exp. (2009) L03004.

[24] M. Horvat, T. Prosen, and G. Casati, Phys. Rev. E **80**, 010102 (2009).

[25] K. Saito, G. Benenti, and G. Casati, Chem. Phys. **375**, 508 (2010).

[26] R. Franzosi, J. Stat. Phys. **143**, 824 (2011).

[27] With a slight abuse of terminology, we use the language of thermoelectric phenomena, even though the underlying physical process is thermodiffusion, since particles have no electric charge in the DNLS context.

[28] Actually, it is possible to model the interaction of a DNLS system with a finite-temperature heat bath by adding multiplicative noise and nonlinear damping, as discussed by P. L. Christiansen, Yu. B. Gaididei, M. Johansson, and K. Ø. Rasmussen, Phys. Rev. B **55**, 5759 (1997). The model there presented conserves the norm but exchanges energy.

[29] B. Rumpf, Physica D **238**, 2067 (2009).

[30] For the sake of simplicity, we refer to the left boundary, but the same rule refers to the Nth site as well.

[31] In general, both T and μ contain additional terms $\tilde{T}$ and $\tilde{\mu}$ that can, however, be neglected. In the DNLS case, it can be proven that $\tilde{T} \equiv 0$, while simulations indicate that $\tilde{\mu} \neq 0$ but also that $\langle \tilde{\mu} \rangle = 0$. Indeed, the value of μ computed ignoring $\tilde{\mu}$ coincides with the expected value when $\mu_L = \mu_R$, $T_L = T_R$. In any case, even in a nonequilibrium setup, μ must be computed on sufficiently long subchains. This choice is particularly delicate for small nonlinearities and low temperatures. For instance, for $T = 0.5, \mu = -0.5$, subchains of at least $10 \div 20$ sites are needed.

[32] S. Iubini, S. Lepri, and A. Politi (unpublished).

[33] Z. Rieder, J. L. Lebowitz, and E. Lieb, J. Math. Phys. **8**, 1073 (1967).

[34] P. Sheng, *Introduction to Wave Scattering, Localization and Mesoscopic Phenomena* (Springer-Verlag, Berlin, 2006), Vol. 88.

[35] A. Dhar and D. Roy, J. Stat. Phys. **125**, 805 (2006).